ADVANCES IN ATMOSPHERIC SCIENCES, VOL. 26, NO. 2, 2009, 253–264

Comparison of Daily Extreme Temperatures over Eastern China and South Korea between 1996–2005

LI Hongmei[1,2] (李红梅), ZHOU Tianjun[*1] (周天军), and Jae-Cheol NAM[3]

[1]*State Key Laboratory of Numerical Modeling for Atmospheric Sciences and Geophysical Fluid Dynamics, Institute of Atmospheric Physics, Chinese Academy of Sciences, Beijing* 100029

[2]*Graduate University of Chinese Academy of Sciences, Beijing* 100049

[3]*Meteorological Research Institute, Korea Meteorological Administration, Seoul* 46018*, Korea*

(Received 1 November 2007; revised 10 June 2008)

ABSTRACT

This paper examined the decadal mean, seasonal cycle, and interannual variations of mean and extreme temperatures using daily temperature and relative humidity data from 589 stations over eastern China and South Korea between 1996–2005. The results show that the decadal mean $T_{\rm m}$ (mean daily mean temperature) and the $\rm TN_n$ (minimum daily minimum temperature) increase from north to south; the opposite spatial gradient is found in the DTR (diurnal temperature range); the value of the DTR over South Korea is in-between that over North China and the mid-low Yangtze River valley; the $\rm TX_x$ (maximum daily maximum temperature) has a unique spatial distribution, with the largest value over eastern China. The highest standard deviation (STD) is located over northern China and the $\rm TN_n$ has the largest area coverage of the high STD. The peak of the seasonal cycle for the $T_{\rm m}$, $\rm TX_x$ and $\rm TN_n$ over South Korea (August) occurs one month later than that over eastern China (July). The seasonal cycle of the DTR has two peaks (April and October); the value in the middle-lower reaches of the Yangtze River valley is larger than that in South Korea during July and August owing to the seasonal northward jump of the major monsoon rain band. The interannual variations of summertime temperature indices including the $T_{\rm m}$, $\rm TX_x$, and DTR over South Korea are consistent (opposite) to that over northern (southern) China. For the wintertime temperature indices however, the variation over South Korea is consistent with that over eastern China.

Key words: extreme temperature indices, decadal mean, seasonal cycle, interannual variation

Citation: Li, H. M., T. J. Zhou, and J.-C. Nam, 2009: Comparison of daily extreme temperatures over eastern China and South Korea between 1996–2005. *Adv. Atmos. Sci.*, **26**(2), 253–264, doi: 10.1007/s00376-009-0253-3.

1. Introduction

Variations of climate extremes are active topics in the climate change research community. Trends in daily precipitation and temperature extremes over China during the last half century were studied by Zhai et al. (1999), Yan and Yang (2000), Qian and Zhu (2001), Gong and Ho (2002), Han and Gong (2003), Zhai and Pan (2003a,b), Gong et al. (2004), Zhai et al. (2005), and Wang and Zhou (2005). These previous studies found trends of a decreasing diurnal temperature range (DTR) and frost days over most parts of China. The indices based on the minimum temperatures increased more significantly and consistently than the maximum temperatures in spatial distribution; the dominant feature of trends in extreme precipitation events is an increase along the Yangtze River valley and a decrease over North China. Analysis employing longer data coverage showed that this warming over China has been occurring since the early 1900s (Qian and Zhu, 2001; Yan et al., 2002), along with a warming trend in the monthly mean surface air temperature (Zhou and Yu, 2006). DeGaetano and Allen (2002) found that the minimum temperature was more easily affected by urbanization than was the maximum temperature. Qian and Lin (2004) also mentioned

*Corresponding author: ZHOU Tianjun, zhoutj@lasg.iap.ac.cn

that the urbanization effects on minimum temperatures might have something to do with the more uniform distribution of trends in the night temperatures rather than the day temperatures in China.

The annual mean temperatures over South Korea also show an upward trend. There are some indications that climatic extremes have increased during recent decades. The DTR has increased in the latter part of the time series (except for summer), as a result of a more rapid increase in maximum temperatures than in minimum temperatures, which is not consistent with results reported elsewhere in the world (Chung and Yoon, 2000; Jung et al., 2002; Ryoo et al., 2004).

Previous studies mainly focused on the long-term trends of extreme indices, which ignored the interannual variation and seasonal cycle. Nearly all of the analyses only employed data prior to the year 2000. Although both China and Korea are located in the eastern part of the Eurasian continent and both are covered by the East Asian monsoon system (Zhou and Li, 2002), previous analyses of climate extremes were performed separately, partly owing to the shortage of data sharing. Benefiting from the joint research program between the Meteorological Research Institute (METRI)/Korea Meteorological Administration (KMA) and the Institute of Atmospheric Physics (IAP)/Chinese Academy of Sciences (CAS), we have the opportunity to address the climate extremes in China and Korea by combing data available from the two countries. The present study aims to answer the following questions: (1) What are the variations in the extreme temperatures over China and South Korea during the last decade? (2) Are there any resemblances between the extreme temperature changes in China and South Korea? We will mainly compare the following three regions: the mid-low Yangtze River valley (28°–31.5°N, 113°–120°E), North China (32.5°–41°N, 113°–120°E), and South Korea (33°–38°N, 124°–130°E). These are typical monsoon regions and have been the research focus of the climate research community (e.g. Zhou and Yu, 2005).

The rest of the paper is organized as follows. We first introduce the data and analysis method in section 2. We then present the results in section 3. A summary associated with a brief discussion is given in section 4.

2. Data and methods

The daily temperature dataset, including the daily mean temperature (T_{mean}), daily maximum temperature (T_{max}), daily minimum temperature (T_{min}), and the relative humidity (RH) covering eastern China and South Korea for the period 1996–2005 are used in this study. The Chinese data was archived at the Climate Data Center of the National Meteorological Center/China Meteorological Administration. The Korean data was provided by METRI/KMA.

The data was quality controlled according to Alexander et al. (2006). The temperature records which are not in the range of −70°C–70°C are set to be a missing value. Both the daily maximum and minimum temperatures are set to a missing value if the daily maximum temperature is smaller than the daily minimum temperature. In this study, for certain days of the year, we archived a temperature range using the climatology mean plus and minus four standard deviations. The daily temperature values outside the range for the day are manually checked. We eliminated those stations with too many missing data points (>5

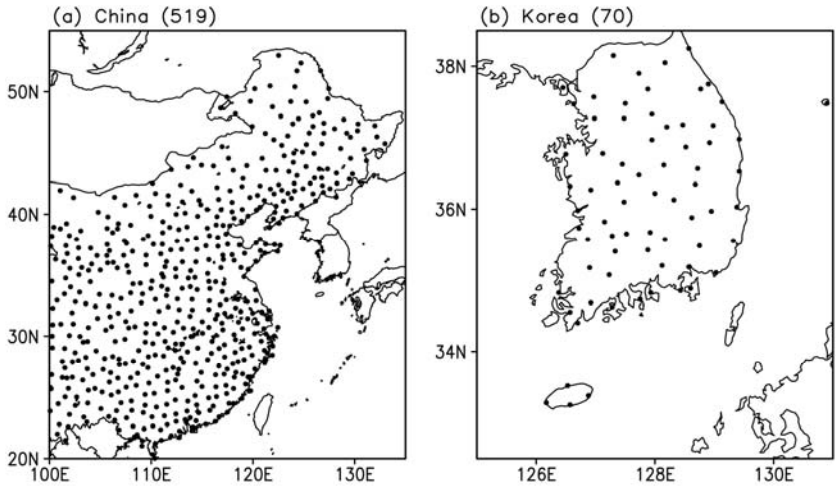

Fig. 1. The location of the stations used in this study, (a) 519 stations over eastern China, (b) 70 stations over South Korea.

d yr^{-1}). Finally, we archived a set of high-quality data from 519 stations over eastern China and 70 stations over South Korea. Figure 1 shows the location of the 519 stations in eastern China and the 70 stations in South Korea used in this study.

Through international coordination, the Expert Team on Climate Change Detection, Monitoring and Indices (ETCCDMI) developed a uniform suite of extreme climate change indices to enable the global analysis of extremes (Alexander et al., 2006). The indices used in this study are: mean $T_{\rm mean}$ (hereafter $T_{\rm m}$), maximum $T_{\rm max}$ (hereafter TX$_{\rm x}$), minimum $T_{\rm min}$ (hereafter TN$_{\rm n}$), and DTR. Among these indices, TX$_{\rm x}$ and TN$_{\rm n}$ represent the extreme conditions as the hottest and coldest day's temperature at the reference time (a month or a year). Considering that extreme temperatures affect our environment as the extreme hot events in summer and extreme cold events in winter, we therefore chose the hottest four months, June–July–August–September, mainly for TX$_{\rm x}$ analyses and the coldest four months, November-December-January-February, mainly for TN$_{\rm n}$ analyses.

The methods used in this study include composite, correlation, and the Empirical Orthogonal Function (EOF) analysis. To extend the length of the time series, we used the monthly data spanning June–July–August–September for the summertime $T_{\rm m}$, TX$_{\rm x}$, DTR, and RH indices and monthly data spanning November–December–January–February for the wintertime $T_{\rm m}$, TN$_{\rm n}$, DTR, and RH during the period 1996–2005. The climatological seasonal cycle was removed from the original data before performing relevant analysis. The correlation method is used to investigate the similarity in the variation between eastern China and South Korea, and the significant level is set to 5% in this study; for two time series with forty months of data each, the threshold value of the significant test is 0.31 at the 5% level.

3. Results

3.1 *Decadal mean*

The decadal mean and standard deviation (hereafter STD) of the annual daily temperature indices over eastern China and South Korea are shown in Fig. 2. The annual $T_{\rm m}$ has a quasi-zonal uniform spatial pattern and increases from north to south. The value of $T_{\rm m}$ over South Korea is a little smaller than that over the same latitude of North China. The STD measures the strength of the interannual variability. As shown in Fig. 2a, the STD over North China, Northeast China, and South Korea is generally larger than 0.5°C. The annual mean $T_{\rm max}$ and $T_{\rm min}$ show a similar spatial pattern as $T_{\rm m}$ (figures not shown), which means that the spatial distribution of the annual mean $T_{\rm max}$ and $T_{\rm min}$ is consistent with $T_{\rm m}$. Do the extreme temperature indices such as TX$_{\rm x}$ and TN$_{\rm n}$, calculated from $T_{\rm max}$ and $T_{\rm min}$ have the same spatial variation with $T_{\rm m}$?

The decadal mean and variation in the extreme temperature indicators are shown in Figs. 2b–c. The annual TX$_{\rm x}$ represents the hottest daytime temperatures through the year (Fig. 2b). Because the annual maximum $T_{\rm max}$ occurred in summer over East Asia, the annual TX$_{\rm x}$ mainly reflects summertime characteristics. Therefore, the spatial distribution of the summertime TX$_{\rm x}$ (not shown) is almost the same as the annual one. Different from the mean temperature indices, we see a larger TX$_{\rm x}$ in regions between 105°E and 120°E, with the highest values over North China. The TX$_{\rm x}$ in South Korea (34°C) is much lower than that in eastern China (36°C), which indicates that there are less hot extreme events in the summer over South Korea than those over eastern China. The STD over northern China (>1.5°C) is larger than other regions, which reflects a large interannual variation of extreme high temperatures in northern China.

The decadal mean and STD of the annual TN$_{\rm n}$ over eastern China and South Korea are shown in Fig. 2c. Because the annual minimum $T_{\rm min}$ occurred in the winter over East Asia, the annual TN$_{\rm n}$ mainly represents winter characteristics. The spatial pattern of the decadal mean TN$_{\rm n}$ is consistent with $T_{\rm m}$, with quasi-zonal distribution, and increases from north to south. In addition, the TN$_{\rm n}$ in the eastern flank of the Tibetan Plateau (Sichuan Basin) is higher than its adjacent area by about 4°C, which indicates that this area has less cold extremes in the winter. South Korea's (−15°C) TX$_{\rm x}$ is a little lower than that over the same latitude of North China, but much lower than the Yangtze River valley (−6°C). Comparing the $T_{\rm m}$ and TX$_{\rm x}$, the TN$_{\rm n}$ has the largest STD, especially for northeast China and South Korea, which indicates their large interannual variations.

From the above analysis, we found that the variations of $T_{\rm max}$ and $T_{\rm min}$ are asymmetric, and therefore showed the decadal mean and STD of the DTR (Fig. 2d). For the humidity difference, the DTR decreases from north to south. Both southwestern China and the coastland have a small DTR. The spatial distribution of RH (not show) is consistent with the DTR; their spatial correlation coefficient reaches −0.74. A larger STD is found over South Korea, northern China, and southeastern China.

3.2 *Seasonal cycle*

In addition to the annual mean conditions, climate extremes over South Korea and eastern China also ex-

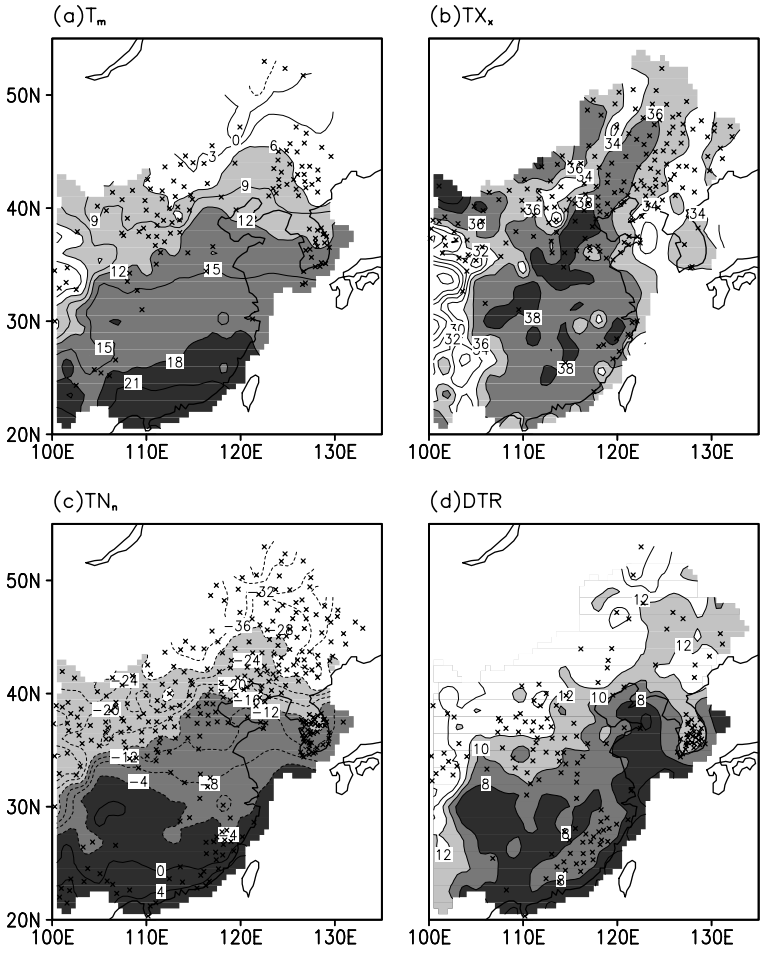

Fig. 2. Decadal mean (contour and shaded) and STD (crosses) of the annual daily temperature indices. (a) T_{m}, (b) $\mathrm{TX_x}$, (c) $\mathrm{TN_n}$, (d) DTR. Crosses in (a) and (d) represent STD larger than 0.5°C, in (b) and (c) represent STD larger than 1.5°C. The shaded area highlights the spatial distribution of decadal mean temperatures.

hibit robust seasonal cycles. Figure 3 shows the seasonal cycle of the regional mean temperature indices in the mid-low Yangtze River valley, North China, and South Korea. The indices include: T_{m} (Fig. 3a), $\mathrm{TX_x}$ (Fig. 3b), $\mathrm{TN_n}$ (Fig. 3c), and DTR (Fig. 3d). Comparing the T_{m} over the three regions, we found that the T_{m} along the mid-low Yangtze River valley is larger than that in the other two regions throughout the year; the T_{m} over North China is larger than that over South Korea from March to July. Different from the seasonal cycle of temperatures along the Yangtze River valley and North China, which peaks in July, the maximum temperature values over South Korea appears in August.

The $\mathrm{TX_x}$ along the mid-low Yangtze River valley is also larger than that in the other two regions. Except for November, December, and January, the $\mathrm{TX_x}$ in North China is larger than that in South Korea. The maximum value of $\mathrm{TX_x}$ appears in June over North China, in July over the mid-low Yangtze River valley, and in August over South Korea. Considering eastern China as a whole, it reaches its maximum $\mathrm{TX_x}$ one month before South Korea, and this phenomenon in the extreme temperature index is consistent with that in the mean temperature index (T_{m}).

The seasonal cycle of the $\mathrm{TN_n}$ is similar to the T_{m}: the mid-low Yangtze River valley has the largest $\mathrm{TN_n}$ value, the $\mathrm{TN_n}$ over South Korea is larger than that over North China in most months. The peak time over South Korea is also one month later than that over the other two regions of eastern China. From the previous analysis, we can see that both the mean and extreme temperatures over eastern China reach their peak one month earlier than that over South Korea.

The DTR has two peaks throughout the year, in April and in October; it appears as a semi-annual cy-

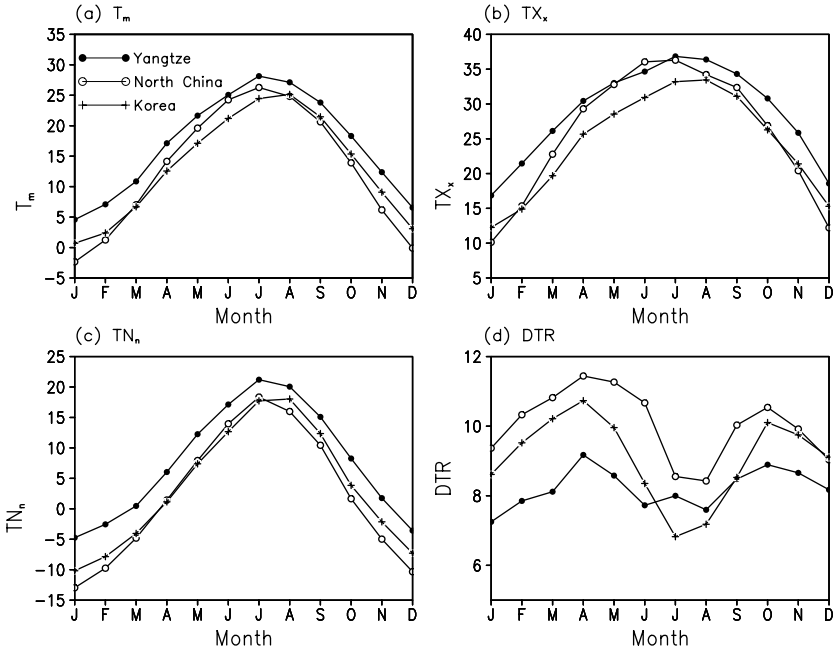

Fig. 3. Seasonal cycle of temperature indicators in the mid-low Yangtze River valley, North China, and South Korea. (a) T_m, (b) TX_x, (c) TN_n, (d) DTR.

Table 1. Correlation coefficients between the regional mean time series of each temperature indice over South Korea (i.e., Fig. 4). Bolded characters indicate statistically significant at the 5% level.

(a)	Summer			
	T_m	TX_x	DTR	RH
T_m	1.00	**0.57**	0.24	−0.07
TX_x	**0.57**	1.00	**0.46**	−0.29
DTR	0.24	**0.46**	1.00	**−0.83**
RH	−0.07	−0.29	**−0.83**	1.00
(b)	Winter			
	T_m	TN_n	DTR	RH
T_m	1.00	**0.73**	0.04	0.51
TN_n	**0.73**	1.00	0.15	0.12
DTR	0.04	0.15	1.00	**−0.32**
RH	0.51	0.12	**−0.32**	1.00

cle, which is consistent over all three regions. In general, North China has the largest value among the three regions, South Korea has the medium value, and the mid-low Yangtze River valley has the smallest DTR. However, the DTR in the mid-low Yangtze River valley is larger than that in South Korea during July and August. The seasonal cycle of DTR is closely related to that of precipitation variations. Following the seasonal cycle of precipitation, which peaks in June along the Yangtze River valley and jumps northward in July (Yu et al., 2000; Zhou and Li, 2002), the corresponding DTR increases in July along the mid-low Yangtze River valley.

3.3 *Inter-annual variations*

To reveal the interannual variation of climate extremes, we calculated multi-station mean temperature and humidity indices over South Korea and present the results in Fig. 4. For T_m, TX_x, DTR, and RH in Fig. 4a, the time series shows monthly anomalies from June–July–August–September for the period 1996–2005. For T_m, TN_n, DTR, and RH in Fig. 4b, the time series shows monthly anomalies from November–December–January–February for the period 1996–2005. A strong interannual variation is seen. The correlation coefficients between every two indices are shown in Table 1a for the summertime. The correlations between TX_x and T_m (0.57), and between TX_x and DTR (0.46) are statistically significant at the 5% level. It indicates that the extreme temperature indices have consistent variations with the mean temperatures. The large correlation coefficient between the DTR and RH (−0.83) confirms their close connection. Table 1b shows the correlation coefficients between each indicator in wintertime; the correlation coefficient between TN_n and T_m (0.73) is much higher than that of the TX_x in summer, and the correlation between T_m and RH reaches 0.51. Although the correlation between DTR and RH (−0.32) is much lower

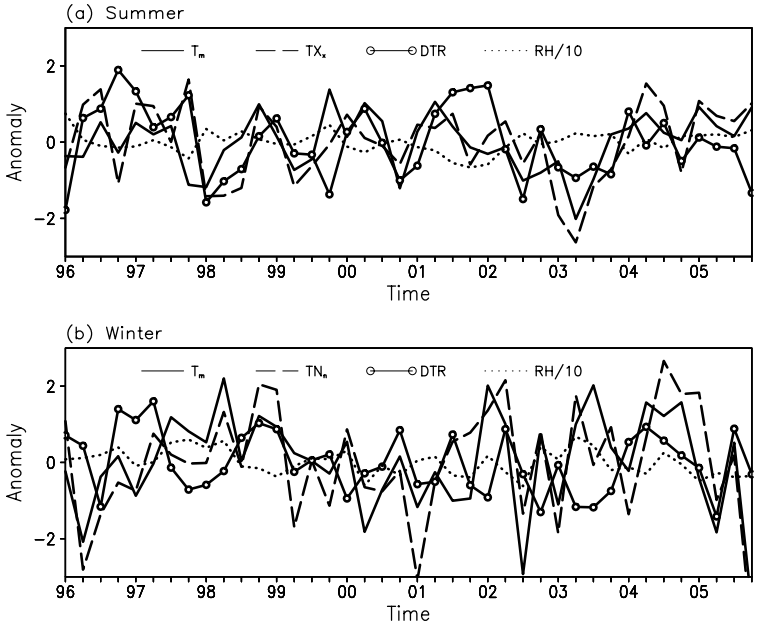

Fig. 4. Time series of multi-station mean temperature indices over South Korea, (a) summer time (June–July–August–September) T_{m}, $\mathrm{TX_x}$, and DTR anomaly, (b) winter time (November–December–January–February) T_{m}, $\mathrm{TN_n}$, and DTR anomaly. The climatology seasonal cycle has been removed.

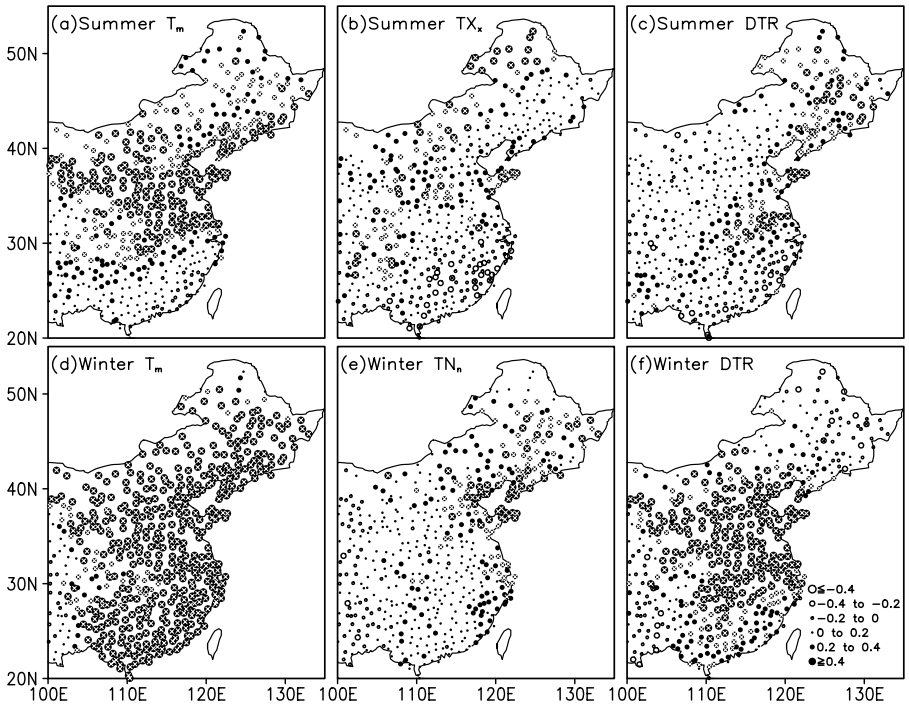

Fig. 5. Spatial pattern of correlation coefficients between regional mean temperature indices over South Korea (Fig. 4) and the temperatures over eastern China. (a) summer T_{m}, (b) summer $\mathrm{TX_x}$, (c) summer DTR, (d) winter T_{m}, (e) winter $\mathrm{TN_n}$, (f) winter DTR. Crosses indicate correlations are statistically significant at the 5% level.

than in summer, it is also significant.

South Korea is located in the region neighboring eastern China. It is desirable to examine whether the changes of extreme temperatures over South Korea are significantly relevant to those over eastern China. To explore the potential resemblances between these two regions, we calculated the correlation coefficients of the temperature anomalies over eastern China with a time series of temperature indices averaged over South Korea. The results are presented in Fig. 5. A significant high positive (negative) correlation is seen over northern China (southeastern China) in the summertime $T_{\rm m}$, $\rm TX_x$, and DTR indices (Figs. 5a–c). For DTR, there is a southwest to northeast oriented belt with significant correlation coefficients, which reflect the effects of the East Asian summer monsoon rainfall. For the wintertime $T_{\rm m}$, $\rm TN_n$, and DTR (Figs. 5d–f), the positive correlation location displays a north to south oriented distribution; the correlation is positive, however, not significant over southeastern China. The largest correlation for $\rm TN_n$ is located over North China, comparing to it the relatively small positive correlation for $\rm TX_x$ over North China. Hence, the temperature change over South Korea is significantly related to that over North China. Compared to that of the mean temperature, the homogenous patterns of extreme temperatures are not so robust.

To further estimate the spatial patterns and interannual variations of temperature, we applied EOF analysis to mean and extreme temperature indices over eastern China and South Korea. Figure 6 shows the spatial pattern of the loading EOF mode and the corresponding principle component (PC) of the normalized June-July-August-September $T_{\rm m}$. The EOF1 explains 30.1% of the total variance. It shows a consistent temperature variation over eastern China and South Korea. The corresponding PC is standardized to have a zero mean and unit variance. Times when the PCs cross the horizontal lines ± 1 are arbitrarily chosen to represent particularly high amplitude or extreme events; the largest negative event occurred in September 1997. Variation of the PC is consistent with the regional mean $T_{\rm m}$ over South Korea (see Fig. 4), showing a simultaneous correlation coefficient of 0.74.

The spatial pattern of the loading EOF mode and

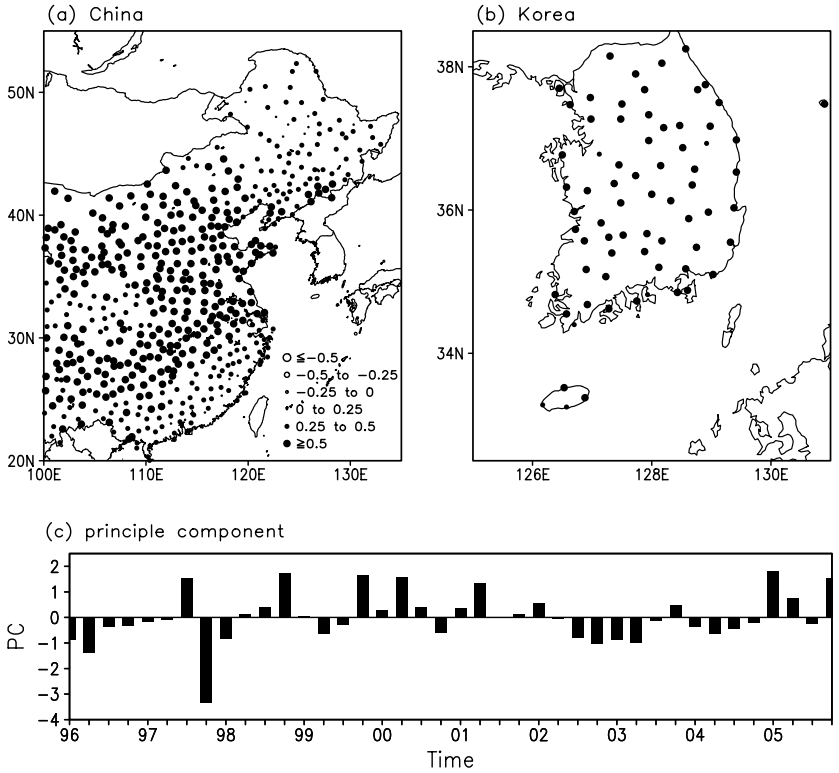

Fig. 6. Spatial pattern of the loading Empirical Orthogonal Function (EOF) mode and corresponding principle component of normalized June-July-August-September $T_{\rm m}$. (a) EOF1 over eastern China, (b) EOF1 over Korea, (c) the principle component. The EOF patterns are shown as the normalized $T_{\rm m}$ regressed upon the corresponding PC time series.

the corresponding principle component of the normalized TX_x is shown in Fig. 7. The EOF1 explains 20.0% of the total variance, which shows positive values over northern China and South Korea, and negative values over southeastern China. It indicates a regions. A tiny negative trend can be found in PC1, with the positive maximum value in 1997 and negative maximum value in 2003. The variation of the PC time series is also consistent with the regional mean TX_x over South Korea (Fig. 4), having a correlation coefficient of 0.59.

The TX_x mainly reflects the summer extreme temperature characteristics. Besides the hot extremes in summer, the variation of cold extremes in winter is also very important. To reveal the winter extreme temperature variations, we apply EOF analysis to wintertime TN_n (Fig. 8). The first EOF mode explains 33.0% of the total variance, which shows consistent variations. However, the positive value over Northeast China and South Korea is much smaller than that over eastern China, so the EOF1 mainly reflects variations over eastern China.

The summertime DTR's EOF1 (21.3%) and corresponding PC1 are similar to the TX_x's, which indicates that the interannual DTR variations are consistent with the TX_x over both eastern China and South Korea (Fig. 9).

The consistent variation of summertime TX_x and DTR over North China, South Korea, and South China are mainly related to the East Asian summer monsoon rainfall. The monsoon brings abundant water vapor to East Asia in the summer; here we showed the variations of RH in Fig. 10. From EOF1 (18.8%) and the corresponding PC1, we can see that it has a similar spatial and temporal distribution to the TX_x (Fig. 7) and DTR (Fig. 9). The wintertime TN_n may be affected by the cold wave and frequent weather system perturbations from higher latitudes.

Based on the time series of PC1 and the regional mean indices over South Korea, we calculated their correlation coefficients, the results are shown in Table 2. The correlation between PC1 and the corresponding South Korean mean time series for T_m, TX_x (TN_n), DTR, and RH is 0.74 (0.77), 0.59 (0.33), 0.51 (0.69), and 0.41 (0.47) in the summertime (wintertime), respectively. This is statistically significant at the 5% level, and hence confirms the coherent changes of climate extremes between eastern China and South Korea. In addition, the correlation between the PC1 of the DTR and the South Korean mean TX_x in the summer is statistically significant at the 5% level, which indicates a consistent variation between DTR and TX_x.

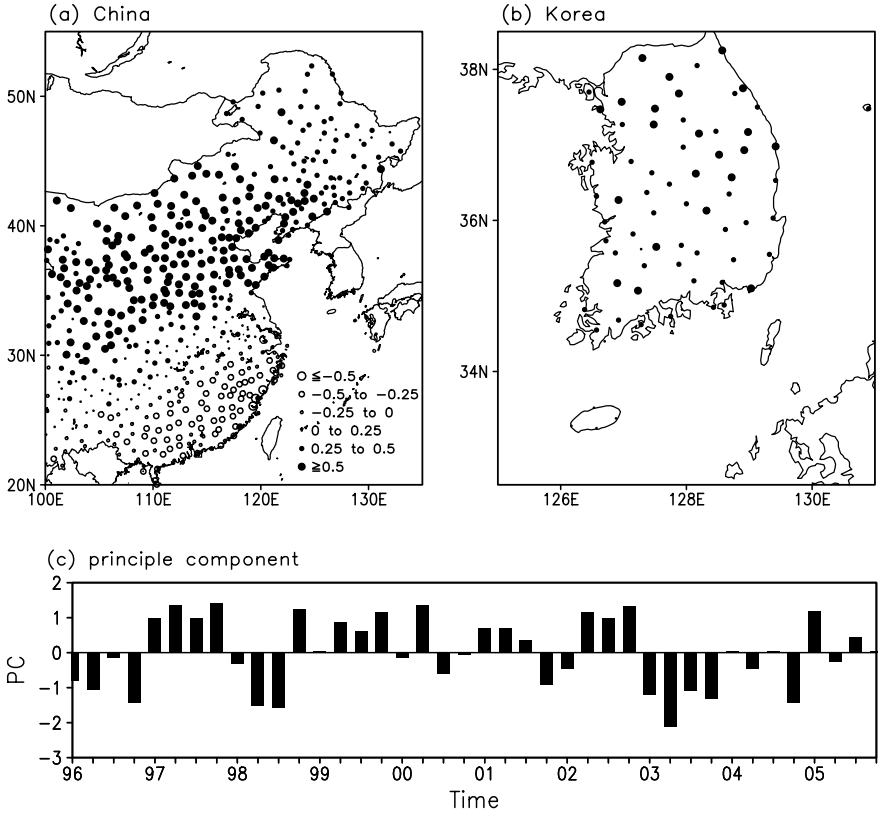

Fig. 7. Same as in Fig. 6, but for TX_x.

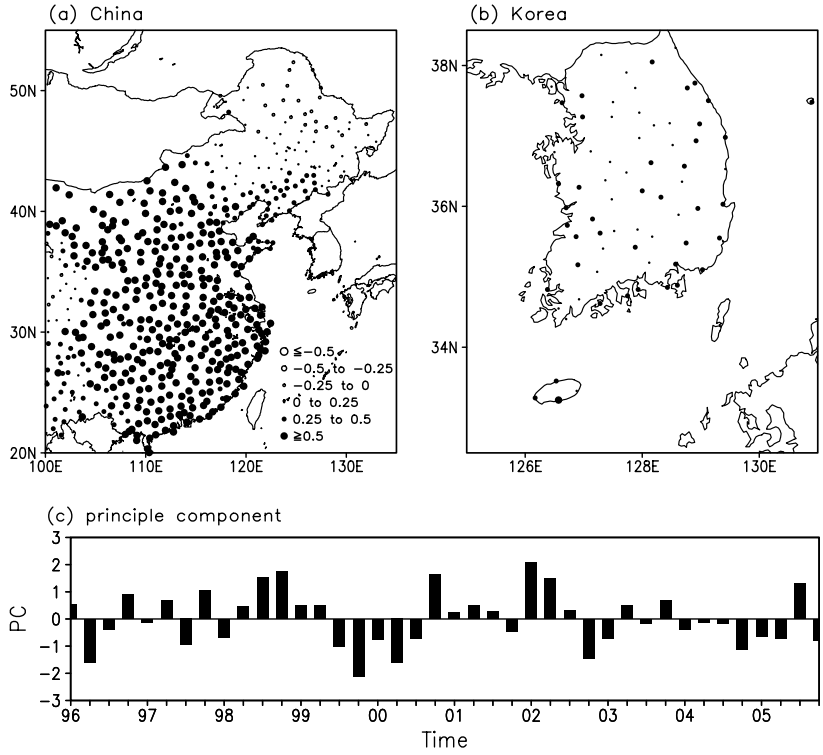

Fig. 8. Same as in Fig. 6, but for November–December–January–February TN_n.

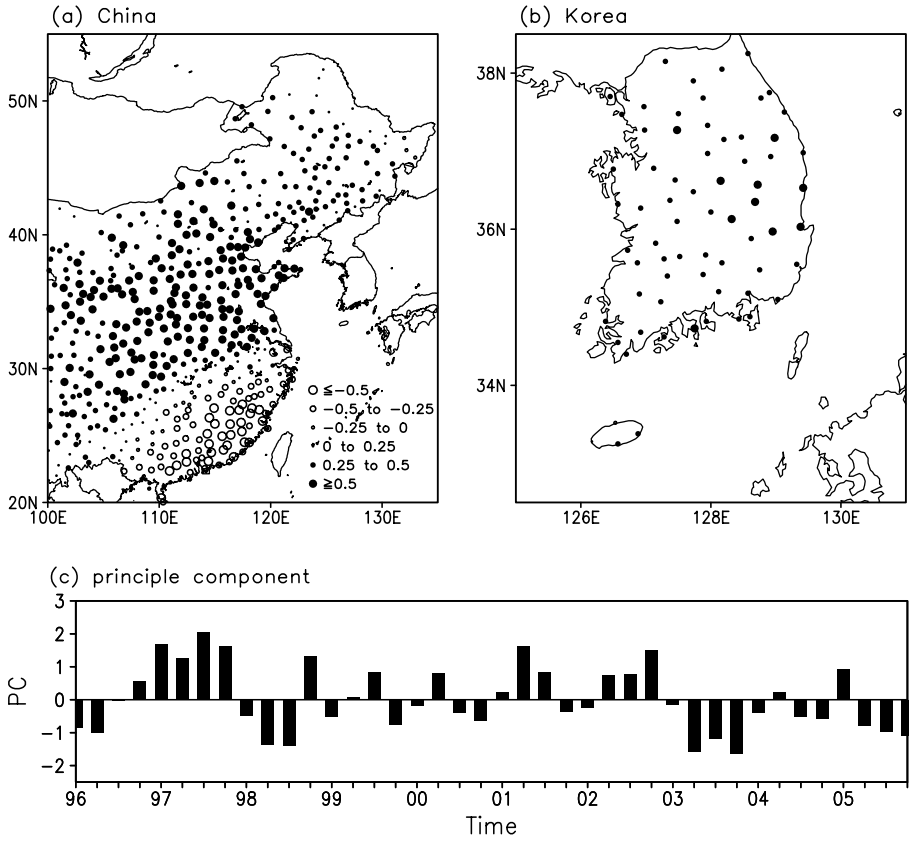

Fig. 9. Same as in Fig. 6, but for DTR.

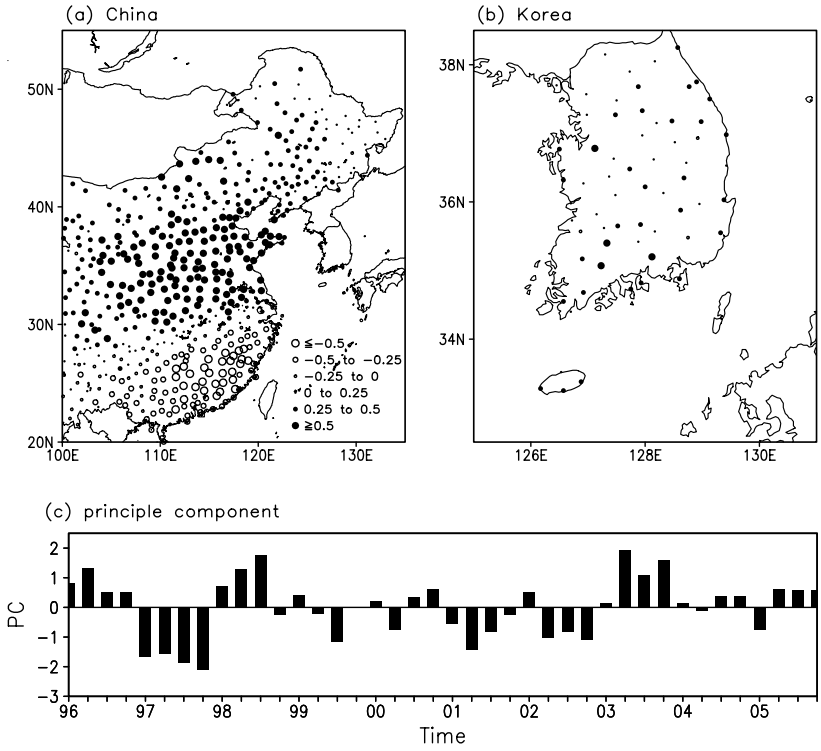

Fig. 10. Same as in Fig. 6, but for RH.

Table 2. Correlation coefficients between PC1 (PC for short in table) (i.e., Figs. 6c–10c) and the time series of temperature indices averaged over South Korea (SK for short in table) (i.e., Fig. 4). Bolded characters indicate statistically significant at the 5% level.

(a)	Summer			
	PC			
SK	T_m	TX_x	DTR	RH
T_m	**0.74**	**0.33**	0.20	−0.23
TX_x	0.11	**0.59**	**0.44**	**−0.48**
DTR	−0.02	0.20	**0.51**	**−0.41**
RH	0.07	−0.19	**−0.41**	**0.41**
(b)	Winter			
	PC			
SK	T_m	TN_n	DTR	RH
T_m	**0.77**	**0.36**	0.06	**0.32**
TN_n	**0.54**	**0.33**	0.01	**0.32**
DTR	**0.35**	0.30	**0.69**	**−0.44**
RH	0.20	−0.04	−0.20	**0.47**

4. Summary and discussion

4.1 *Summary*

Using daily temperature and relative humidity data from 589 stations covering eastern China and South Korea during the period 1996–2005, we have examined the decadal mean, the seasonal cycle, and interannual variations in mean and extreme temperature indices and their potential relationship to humidity. The major results are summarized as follows.

(1) The decadal mean T_m and TN_n increase from north to south with a quasi-zonal spatial distribution. The TX_x, however, has unique spatial distributions, with the largest value over eastern China. Due to humidity differences, DTR decreases from north to south. The T_m, TX_x, and TN_n over South Korea is much lower than those over eastern China, and the value of DTR over South Korea is in between that over North China and the mid-low Yangtze River valley. The largest interannual variation of mean and extreme temperature indices is located over northern China.

(2) For the seasonal cycle of the regional mean temperature indices over the mid-low Yangtze River valley, North China, and South Korea, both the mean and extreme temperatures along the mid-low Yangtze River valley are larger than those over the other two regions year-round. The peak of the seasonal cycle for T_m, TX_x, and TN_n over South Korea (August) occurs one month later than in eastern China (July). The seasonal cycle of DTR has two peaks (April and October). In general, North China has the largest value among the three regions, South Korea has the medium

value, and the mid-low Yangtze River valley has the smallest. However, the DTR in the mid-low Yangtze River valley is larger than that in South Korea during July and August owing to the northward jump of the monsoon rain belt in July.

(3) The time series of multi-station mean temperature indices over South Korea exhibit significant interannual variations. Owing to the effects of the East Asian summer monsoon rain belt, the interannual variations of the summertime temperature indices including $T_{\rm m}$, $\rm TX_x$, and DTR over South Korea are consistent (opposite) to that over North (South) China. For the wintertime temperature indices, however, the variation over South Korea is consistent with that over eastern China. In general, the interannual temperature variations over South Korea are consistent with those over North China. The significant correlation between the regional mean time series over South Korea and PC1 of the EOF analysis over eastern China and South Korea for a certain temperature index indicates the spatial continuity of temperature variations.

4.2 *Discussion*

In terms of the seasonal cycle, the time when South Korea reaches its maximum value is different from that of eastern China, however, both the correlation analysis and the EOF analysis on the interannual variability show that the temperature variations over South Korea are consistent with those over North China. In recent decades, a marked summer precipitation change (often called the 'Southern-flooding-and-Northern-drought' pattern) has been observed in eastern China. Precipitation has increased over the middle and lower reaches of the Yangtze River valley, whereas it has decreased over the middle to lower reaches of the Yellow River valley (Hu et al., 2003; Yu et al., 2004; Yu and Zhou, 2007). A recent examination shows that the excessive rain belt extends from the middle-to-lower Yangtze River valley across the East China Sea and South Korea to northern Japan, signaling consistent variations of climate between South China and South Korea (Wang et al., 2006). This result is different from the interannual variations of temperature shown above, which reveals a coherent change of temperatures over North China and South Korea. The reason for this difference warrants further study. Special efforts should be devoted to the potential coherent variations of extreme precipitation over China and South Korea. By combing data available from the East Asian countries, we wish to develop an integral view of the changes of climate extremes across the entire eastern Asian region in the near future.

Acknowledgements. This paper contributes to the joint research program between the Institute of Atmospheric Physics (IAP)/Chinese Academy of Sciences (CAS) and the Meteorological Research Institute (METRI)/Korea Meteorological Administration (KMA). This work was jointly supported by the Natural Science Foundation of China (NSFC) under Grant Nos. 40523001, 40625014, 40221503, and the National Basic Research Program of China (2005CB321703). We thank Ms. Judith Aplon for providing assistance in editing the English. The helpful suggestions from the two anonymous reviewers are also gratefully acknowledged.

REFERENCES

Alexander, L., and Coauthors, 2006: Global observed changes in daily climate extremes of temperature and precipitation. *J. Geophys. Res.*, **111**(D05109), 1–22.

Chung, Y., and M. Yoon, 2000: Interpretation of recent temperature and precipitation trends observed in Korea. *Theor. Appl. Climatol.*, **67**, 171–180.

DeGaetano, A., and R. Allen, 2002: Trends in twentieth-century extremes across the United States. *J. Climate*, **15**, 3188–3205.

Gong, D., and C. Ho, 2002: Shift in the summer rainfall over the Yangtze River valley in the late 1970s. *Geophys. Res. Lett.*, **29**(10), 1436, doi: 10.1029/2001GL014523.

Gong, D., Y. Pan, and J. Wang, 2004: Changes in extreme daily mean temperatures in summer in eastern China during 1955-2000. *Theor. Appl. Climatol.*, **77**, 25–37.

Han, H., and D. Gong, 2003: Extreme climate events over northern China during the last 50 years. *Journal of Geographical Sciences*, **13**(4), 469–479.

Hu, Z., S. Yang, and R. Wu, 2003: Long-term climate variations in China and global warming signals. *J. Geophys. Res.*, **108**(4614), doi: 10.1029/2003JD003651.

Jung, H., Y. Choi, J. Oh, and G. Lim, 2002: Recent trends in temperature and precipitation over South Korea. *International Journal of Climatology*, **22**, 1327–1337.

Qian, W., and X. Lin, 2004: Regional trends in recent temperature indices in China. *Climate Research*, **27**, 119–134.

Qian, W., and Y. Zhu, 2001: Climate change in China from 1880 to 1998 and its impact on the environmental condition. *Climatic Change*, **50**, 419–444.

Ryoo, S., W. Kwon, and J. Jhun, 2004: Characteristics of wintertime daily and extreme minimum temperature over South Korea. *International Journal of Climatology*, **24**, 145–160.

Wang, B., Q. Ding, and J. Jhun, 2006: Trends in Seoul (1778–2004) summer precipitation. *Geophys. Res. Lett.*, **33**(L15803), doi: 10.1029/2006GL026418.

Wang, Y., and L. Zhou, 2005: Observed trends in extreme precipitation events in China during 1961-2001 and the associated changes in large-scale circulation. *Geophys. Res. Lett.*, **32**(L09707), doi:

10.1029/2005GL022574.

Yan, Z., and C. Yang, 2000: Geographic pattern of extreme climate changes in China during 1951–1997. *Climatic and Environmental Research*, **5**(3), 267–272. (in Chinese)

Yan, Z., and Coauthors, 2002: Trends of extreme temperatures in Europe and China based on daily observations. *Climatic Change*, **53**, 355–392.

Yu, R., W. Li, X. Zhang, Y. Yu, H. Liu, and T. Zhou, 2000: Climatic features related to eastern China summer rainfalls in the NCAR CCM3. *Adv. Atmos. Sci.*, **17**, 503–518.

Yu, R., B. Wang, and T. Zhou, 2004: Tropospheric cooling and summer monsoon weakening trend over East Asia. *Geophys. Res. Lett.*, **31**(L22212), doi: 10.1029/2004GL021270.

Yu, R., and T. Zhou, 2007: Seasonality and three-dimensional structure of the interdecadal change in East Asian monsoon. *J. Climate*, **20**, 5344–5355.

Zhai, P., A. Sun, F. Ren, X. Liu, B. Gao, and Q. Zhang, 1999: Changes of climate extremes in China. *Climatic Change*, **42**, 203–218.

Zhai, P., and X. Pan, 2003a: Change in extreme temperature and precipitation over Northern China during the second half of the 20th century. *Acta Geographica Sinica*, **58**(suppl.), 1–10. (in Chinese)

Zhai, P., and X. Pan, 2003b: Trends in temperature extremes during 1951–1999 in China. *Geophys. Res. Lett.*, **30**(17), doi: 10.1029/2003GL018004.

Zhai, P., X. Zhang, H. Wan, and X. Pan, 2005: Trends in total precipitation and frequency of daily precipitation extremes over China. *J. Climate*, **18**, 1096–1108.

Zhou, T., and Z. Li, 2002: Simulation of the East Asian summer monsoon by using a variable resolution atmospheric GCM. *Climate Dyn.*, **19**, 167–180.

Zhou, T., and R. Yu, 2005: Atmospheric water vapor transport associated with typical anomalous summer rainfall patterns in China. *J. Geophys. Res.*, **110**, D08104, doi: 10.1029/2004JD005413.

Zhou, T., and R. Yu, 2006: Twentieth century surface air temperature over China and the Globe simulated by coupled climate models. *J. Climate*, **19**(22), 5843–5858.